

Modeling of L-mode plasma intrinsic rotation in ASDEX Upgrade

I. Erofeev, E. Fable, C. Angioni, W. Hornsby, R.M. McDermott and the ASDEX Upgrade Team

Max-Planck-Institut für Plasmaphysik, Garching, Germany

Introduction

Ohmic plasma discharges in tokamaks exhibit a rich phenomenology with complex parameter dependences and present a challenging area for theoretical description. A lot of recent attention has been drawn to the observed in many machines establishment of plasma toroidal rotation in the absence of any external source of momentum. This intrinsic plasma rotation has been found to develop a significant velocity gradient around mid-radius with the increase of collisionality, with high counter-current velocity in the core. However, at even higher collisionality the velocity profile relaxes back to roughly flat. It can be shown that such behavior can only arise from a component of the stress tensor (referred to as the residual stress) not related to either viscosity or convection, which appears when the plasma poloidal symmetry is broken. Many symmetry breaking mechanisms have been proposed recently [1, 2]. Several local mechanisms have been tested with AUG parameters and found to be weak [3], hence a global mechanism is believed to dominate. We assume the most prominent global effect to be the finite poloidal tilting of turbulent eddies due to the radial shearing of background equilibrium profiles [4]. This gives rise to a finite poloidally averaged parallel wave number \hat{k}_{\parallel} that generates the residual stress. The main aim of this work is to estimate the tilt angle $\hat{\theta}_0$ values that suffice to explain the observed toroidal rotation profiles assuming the profile shearing is the only symmetry breaking mechanism, though a consequent flow shearing is also accounted for.

We use the ASTRA transport code [5, 6], coupled to the TGLF transport model [7] and the drift-kinetic solver NEO [8]. We model real ASDEX Upgrade discharges, where the rotation profiles are measured with CXRS [9], covering two plasma current values, $I_p = 0.62$ MA and $I_p = 1.04$ MA, and a range of electron densities. In the simulations, the profiles of current density, electron and ion temperatures evolve consistently with the related transport coefficients until an equilibrium is reached. We fix the electron density profile to experimental, as having exact density gradients is of great importance, whereas with fully self-consistent evolution the results slightly differ from the measurements, especially at low densities. We include boron as single impurity species, with density defined by experimental scaling for the effective charge, $Z_{\text{eff}} = 1 + 3.2I_p^3/\bar{n}_e^3$ (I_p in MA, n_e in $10^{19}m^{-3}$). In the momentum transport simulations the impurity concentration profile is assumed flat, this is then verified with separate impurity transport simulations. Such amount of attention to the impurity content is paid due to its effect on turbulence, especially ITG, which has been shown previously [10].

In the ASTRA equation for radial transport of toroidal momentum [11], we keep both the diffusion and convection terms:

$$\left\langle R \frac{B_\varphi}{B} \Pi_\rho |\nabla \rho| \right\rangle = \frac{R_0^2 B_0}{I} \langle |\nabla \rho|^2 \rangle \left[-\rho_m \chi_\varphi \frac{\partial u}{\partial \rho} + \rho_m V u \right] + \left\langle R \Pi_{\varphi\rho}^{res} |\nabla \rho| \right\rangle$$

The residual stress term can be derived from a fluid model (see [4, 12]) in the form:

$$\Pi_{\varphi\rho}^{res} = \rho_m \chi_\varphi \frac{v_{th,i}}{R^2} \hat{k}_\parallel \left[\frac{R}{L_n} - \frac{4}{\tau} (\hat{k}_\parallel^2 - 1) \right],$$

and the parallel wavenumber can be seen as $\hat{k}_\parallel = 2\hat{\theta}_0 \frac{\hat{s}}{q} \frac{1}{k_y \rho_i}$. In our modeling, however, the poloidally averaged parallel wavenumber \hat{k}_\parallel and the residual stress $\Pi_{\varphi\rho}^{res}$ are produced by TGLF upon providing a tilt angle for its quasi-linear turbulent spectrum. This angle can be computed in non-linear global gyrokinetic simulations.

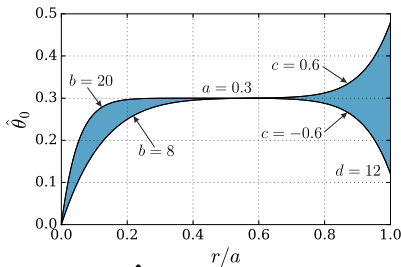


Fig. 1: $\hat{\theta}_0$ parametrization

Several such GKW [13] runs have been performed [14], that showed values of $\hat{\theta}_0$ in the range $0 - 0.4$ and $\hat{k}_\parallel \leq 0.2$ for the plasma parameters corresponding to the 1.04 MA case. On this basis a parametrisation scheme for the tilt angle is proposed, representing it as $\hat{\theta}_0(\rho) = a [1 - (1 - \rho)^b + c\rho^d]$, see

Fig. 1. The tilting effect does not change upon variation of the $\hat{\theta}_0$ profile within the shaded areas, hence we will define the tilt angle as an average value over $r/a = 0.4 - 0.6$, which equals to the a coefficient. We set $b = 8$ and for simplicity $c = 0$.

Momentum transport simulations results

Fig. 2 presents three typical toroidal rotation profiles as measured (dashed) and simulated (solid) at low density (low gradient), intermediate density (high gradient) and high density (low gradient again), as well as the simulated normalized rotation gradient as a function of the density, at $I_p = 1.04$ MA. Positive direction is co-current.

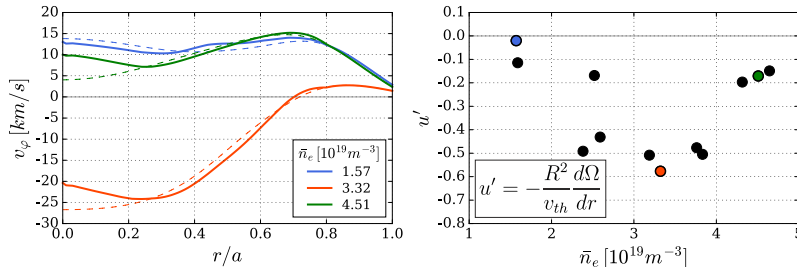


Fig. 2: Rotation profiles and normalized gradients.

The corresponding symmetry breaking parameters, namely $\hat{\theta}_0$, \hat{k}_\parallel and the RS are shown in Fig. 3 (a, c and d), represented by their averages over $r/a = 0.4 - 0.6$. A correlation of the tilt angle with the normalized density gradient is observed (Fig. 3, b). The absolute values of $\hat{\theta}_0$, \hat{k}_\parallel and $\Pi_{\varphi\rho}^{res}$, as well as their profile shapes (Fig. 3, e, f) are in good agreement with GKW

results [14], that supports validity of these results. In contrast to the simple fluid model, relations $\hat{k}_{\parallel}(\hat{\theta}_0)$ and $\Pi_{\phi\rho}^{res}(\hat{k}_{\parallel})$ are not always linear.

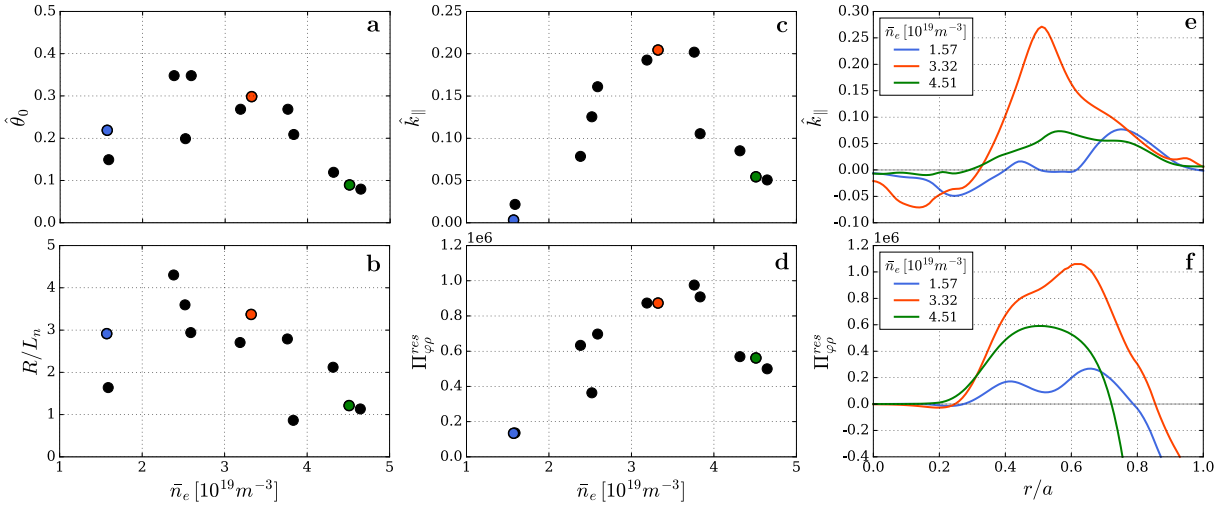


Fig. 3: Asymmetry parameters.

Fig. 4 shows the dependence of the mid-radius averaged u' (a), χ_i (b), the parallel wave vector \hat{k}_{\parallel} (c) and $\Pi_{\phi\rho}^{res}$ (d), as well as the profiles of \hat{k}_{\parallel} (e) and $\Pi_{\phi\rho}^{res}(\hat{k}_{\parallel})$ (f), on the tilt angle, with the density profile fixed (the red data point in Fig. 2 and 3). When $\hat{\theta}_0 \geq 0.3$, \hat{k}_{\parallel} saturates, while the RS exhibits a fast growth and the χ_e , χ_i (and so χ_{ϕ}) decrease rapidly, which leads to an abrupt acceleration of the plasma core. The required values are located close to the bifurcation point. If we set the rotation profile to the experimental value but keep $\hat{\theta}_0$ (dashed black line in the plots), the $E \times B$ shear effect alone is found to provide some reduction in χ_i , as well as a substantial contribution to the residual stress. Despite the significant decrease in heat diffusivities, the temperatures show only a slight growth (like core T_i in Fig. 4, b).

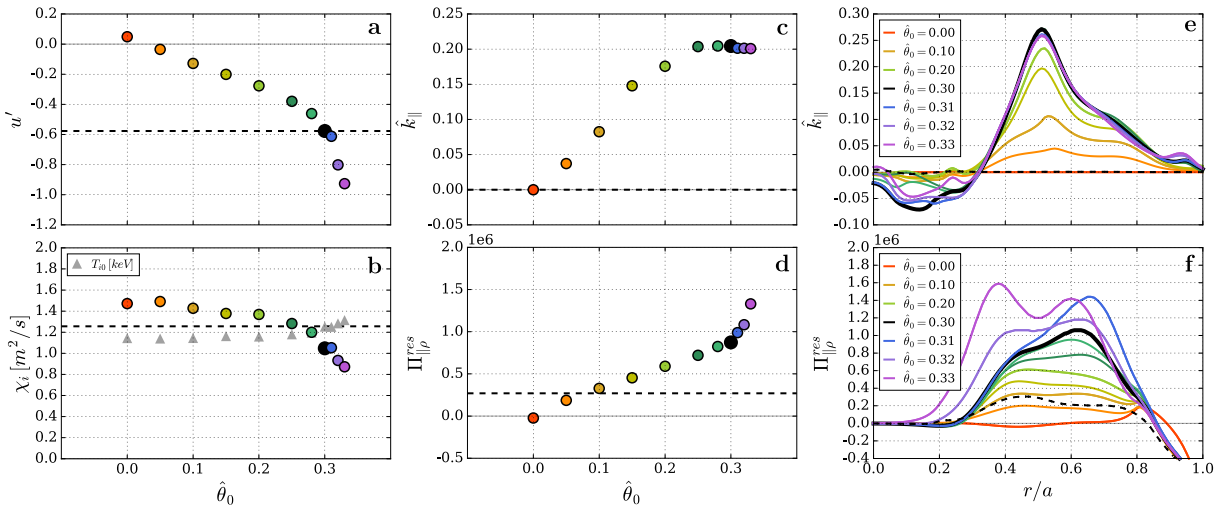


Fig. 4: Theta dependence.

The same picture can be drawn from the analysis of 0.62 MA discharges, with the u' roll-over shifted to lower density and with values up to $u' = -0.8$.

Impurity transport simulations results

The boron transport for the same discharges involved fully self-consistent evolution of electron and ion temperatures, as well as electron and boron densities. The boron source was adjusted for each data point so that the average Z_{eff} equals to the experimental scaling. The resulting boron density profile and the boron concentration profile for the case with $I_p = 1.04$ MA are shown in Fig. 5 (a, b). At low density, more impurity is accumulated at the edge, leading to a concentration profile with $\approx 30\%$ hollowness, see Fig. 5, c. As the electron density increases, boron distributes more uniformly, and at $\bar{n}_e \geq 4 \times 10^{19} m^{-3}$ its concentration is effectively flat. In the plasmas with $I_p = 0.62$ MA such uniformity is reached already at $\bar{n}_e \geq 2.2 \times 10^{19} m^{-3}$.

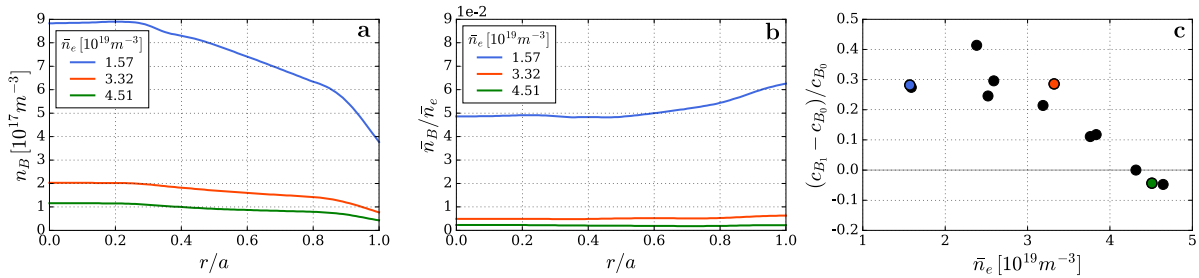


Fig. 5: Simulated boron density and concentration.

Conclusions

We show that the profile shearing mechanism is able to explain the observed toroidal rotation profiles in AUG L-mode plasmas with the assumption of tilt angles in a reasonable range. The values required by TGLF to reproduce the experimental intrinsic rotation profiles are consistent with those from non-linear global GKW runs. The dependence of $\hat{\theta}_0$ on the plasma conditions such as the average density or its gradient, remains to be understood. The relations between $\hat{\theta}_0$, \hat{k}_{\parallel} and the RS are demonstrated to be not linear. We also show a reduction in the heat and momentum (if assume no $Pr(\bar{n}_e)$ dependence) diffusivities, though the temperatures do not vary much. The impurity transport simulations demonstrated low hollowness of boron concentration profiles, that validates the use of flat Z_{eff} profile approximation.

References

- [1] A.G. Peeters *et al.*, Nucl. Fusion **51**, 094027 (2011)
- [2] P.H. Diamond *et al.*, Nucl. Fusion **53**, 104019 (2013)
- [3] W. Horsby *et al.*, Nucl. Fusion **57**, 046008 (2017)
- [4] Y. Camenen *et al.*, Nucl. Fusion **51** 073039 (2011)
- [5] G.V. Pereverzev and Y. P. Yushmanov, IPP Report 5/42 (1991)
- [6] E. Fable *et al.*, Plasma Phys. Control. Fusion **55**, 12402 (2013)
- [7] G.M. Staebler *et al.*, Phys. Plasmas **12**, 102508 (2005)
- [8] E.A. Belly, J. Candy, Plasma Phys. Control. Fusion **50**, 095010 (2008)
- [9] R. M. McDermott *et al.*, Nucl. Fusion **54**, 043009 (2014)
- [10] I. Erofeev *et al.*, submitted to Nucl. Fusion (2017)
- [11] E. Fable, Plasma Phys. Control. Fusion **57**, 045007 (2015)
- [12] A.G. Peeters *et al.*, Phys. Plasmas **16**, 042310 (2009)
- [13] A.G. Peeters *et al.*, Comput. Phys. Commun. **180**, 2650 (2009)
- [14] W.A. Hornsby, EPS 2017 poster